

Improved crystal quality and performance of GaN-based light-emitting diodes by decreasing the slanted angle of patterned sapphire

Ji-Hao Cheng, YewChung Sermon Wu, Wei-Chih Liao, and Bo-Wen Lin

Citation: *Applied Physics Letters* **96**, 051109 (2010); doi: 10.1063/1.3304004

View online: <http://dx.doi.org/10.1063/1.3304004>

View Table of Contents: <http://scitation.aip.org/content/aip/journal/apl/96/5?ver=pdfcov>

Published by the [AIP Publishing](#)

Articles you may be interested in

[The improvement of GaN-based light-emitting diodes using nanopatterned sapphire substrate with small pattern spacing](#)

AIP Advances **4**, 027123 (2014); 10.1063/1.4867091

[282-nm AlGaIn-based deep ultraviolet light-emitting diodes with improved performance on nano-patterned sapphire substrates](#)

Appl. Phys. Lett. **102**, 241113 (2013); 10.1063/1.4812237

[The aspect ratio effects on the performances of GaN-based light-emitting diodes with nanopatterned sapphire substrates](#)

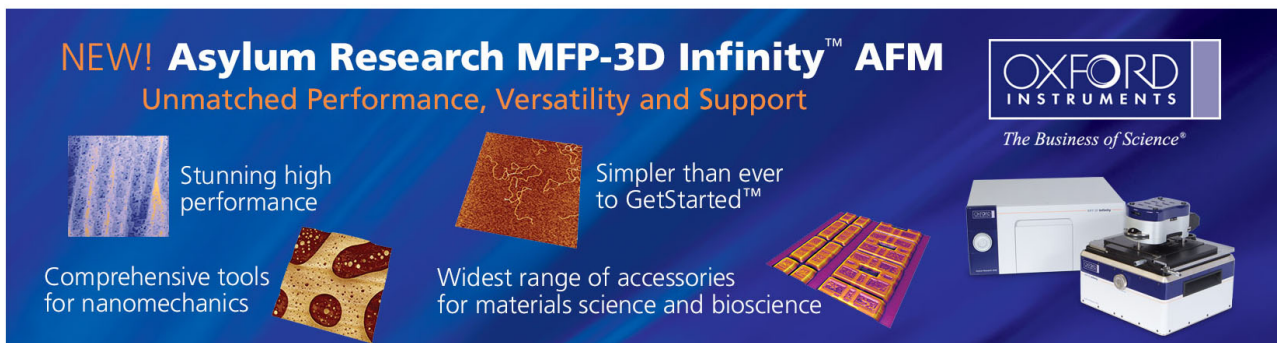
Appl. Phys. Lett. **97**, 023111 (2010); 10.1063/1.3463471

[Enhanced performance of GaN-based light emitting diode with isoelectronic Al doping layer](#)

J. Appl. Phys. **105**, 064508 (2009); 10.1063/1.3095486

[Enhanced light output from aligned micropit InGaIn-based light emitting diodes using wet-etch sapphire patterning](#)

Appl. Phys. Lett. **90**, 131107 (2007); 10.1063/1.2714203



NEW! Asylum Research MFP-3D Infinity™ AFM
Unmatched Performance, Versatility and Support

OXFORD INSTRUMENTS
The Business of Science®

Stunning high performance

Simpler than ever to GetStarted™

Comprehensive tools for nanomechanics

Widest range of accessories for materials science and bioscience

Improved crystal quality and performance of GaN-based light-emitting diodes by decreasing the slanted angle of patterned sapphire

Ji-Hao Cheng,¹ YewChung Sermon Wu,^{1,a)} Wei-Chih Liao,¹ and Bo-Wen Lin^{1,2}

¹Department of Materials Science and Engineering, National Chiao Tung University, Hsinchu 300, Taiwan

²Sino-American Silicon Products Inc., Hsinchu 300, Taiwan

(Received 21 October 2009; accepted 11 January 2010; published online 2 February 2010)

Periodic triangle pyramidal array patterned sapphire substrates (PSSs) with various slanted angles were fabricated by wet etching. It was found beside normal wurtzite GaN, zinc blende GaN was found on the sidewall surfaces of PSS. The crystal quality and performance of PSS-LEDs improved with decrease in slanted angle from 57.4° to 31.6°. This is because most of the growth of GaN was initiated from *c*-planes. As the growth time increased, GaN epilayers on the bottom *c*-plane covered these pyramids by lateral growth causing the threading dislocation to bend toward the pyramids.

© 2010 American Institute of Physics. [doi:10.1063/1.3304004]

Many techniques have been developed for improving the GaN-based light-emitting diodes (LEDs) internal quantum efficiency (IQE) and light extraction efficiency (LEE), such as low temperature buffer layer,¹ epitaxial lateral overgrowth (ELOG),^{2,3} surface roughening,^{4,5} nanoimprinting,⁶ metal mirror reflect layer⁷ and patterned sapphire substrate (PSS).^{8–11} Currently, the PSS technique has attracted much attention for its high production yield. Using the PSS technique can improve both IQE and LEE.

In this study, periodic triangle pyramidal array PSSs with various slanted angles were fabricated by wet etching. The pattern morphology, epilayers quality, microstructure, as well as optical properties of the InGaN/GaN-LED were systematically investigated.

PSSs with periodic patterns (2 μm width and 2 μm spacing) were prepared by standard photolithography. A 100 nm thick SiO₂ film served as the wet-etching hard mask and was deposited on the sapphire surface. As shown in Fig. 1 and Table I, four kinds of periodic triangle pyramidal arrays were etched in hot H₃PO₄-based solutions for various times.^{12,13} They were denoted as A, B, C, and D-PSS.

Their confocal microscope images are shown in Fig. 1. The heights of pyramids were all about 1.20 μm. The structure of A-PSS comprises of a triangle pyramid covered with three {10 $\bar{1}2$ }*r*-planes with a flat top *c*-plane. The slanted angle between the *r*-plane and *c*-plane was 57.4° as listed in Table I. The other PSSs comprise of triangle pyramids covered with different {10 $\bar{1}x$ } (*x* > 2) planes without top *c*-plane. The slanted angle between the *c*-plane and {10 $\bar{1}x$ } planes of samples A, B, C, and D were 57.4°, 45.3°, 38.3°, and 31.6°, respectively. These slanted angles were measured using focus ion beam (FIB) and cross section scanning electron microscopy (SEM) images.

After the clean process, the LED structures were grown by metalorganic chemical vapor deposition. The structures comprised a buffer layer on the PSS, a undoped-GaN layer film, a *n*-GaN layer, a Si-doped AlGaIn cladding layer, an InGaIn-GaN multiple quantum well (MQW) with emission

wavelength in the blue region (450 nm), a Mg-doped AlGaIn cladding layer and a *p*-GaN layer.

The device mesa with a chip size of 350 × 350 μm² was then defined by an inductively coupled plasma to remove Mg-doped GaN layer and MQW until the Si-doped GaN layer was exposed. After annealed at 600 °C for 10 min, the indium tin oxide (ITO) layer was deposited to form a *p*-side contact layer and a current spreading layer. The Cr/Au layer was deposited onto the ITO layer to form the *p*-side and *n*-side electrodes.

The uniformity of device performance is addressed by the wafer mapping of dominant wavelength and forward voltage. The data are obtained at a forward current of 20 mA and with a sampling rate of 180:1, i.e., ~100 devices, across a 2 inch wafer. The average wavelength and forward voltage across the wafer is 448.0 nm and 3.30 V, respectively. The standard deviations of dominant wavelength and forward voltage are 2.5 nm and 0.03 V for all samples.

The average luminescence intensity and the output power of LEDs were listed in Table I. As can be seen, the performance of PSS-LEDs increased with decrease in slanted angle. When the angle decreased to 31.6°, the light intensity and the output power of D-LED were 140.0 mcd and 20.8 mW, which were 1.54 and 1.37 times higher than those of A-LED. This indicates that IQE, GaN crystal quality and LEE improved with decrease in slanted angle.

Light output measurements were conducted at various temperatures, the room temperature IQE values listed were determined by assuming 100% IQE at low temperature

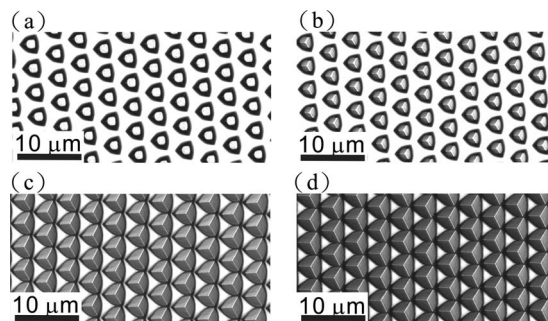


FIG. 1. Confocal microscopy images of PSS: (a) A-PSS, (b) B-PSS, (c) C-PSS, and (d) D-PSS.

^{a)} Author to whom correspondence should be addressed. Electronic mail: sermonwu@stanfordalumni.org. Tel.: 886-3-5131555. FAX: 886-3-5724727.

TABLE I. The parameters and performances of PSS-LEDs.

	Patterned sapphire substrate			GaN on PSS			Light-emitting diodes		
	Pyramid protrusion			XRD FWHM (arcsec)			Average intensity (mcd)	Output power (mW)	η_{int} (%)
	Etched depth (μm)	<i>c</i> -area ratio (%)	Slanted angle ($^\circ$)	(002)	(102)	EPD ($\times 10^7 \text{ cm}^{-2}$)	RT, 20 mA		
A-PSS	1.20	59.6	57.4	269.3	410.3	4.31	91.2	15.2	56.5
B-PSS	1.20	47.5	45.3	264.1	353.6	1.11	121.6	17.2	60.7
C-PSS	1.20	21.6	38.3	251.5	312.6	0.87	131.2	18.5	61.6
D-PSS	1.20	9.6	31.6	243.4	301.2	0.52	140.0	20.8	66.1

(77 K). The measured IQEs (η_{int}) of PSS-LEDs were listed in Table I. The IQE of PSS-LEDs increased with decrease in slanted angle. When the angle decreased to 31.6° , the IQE of D-LED were 66.0%, which was 1.17 times higher than that of A-LED.

Transmission electron-microscopy (TEM) and high-resolution transmission electron microscopy (HRTEM) were used to verify the nature of GaN crystals. Low-magnification cross-sectional TEM images of GaN grown on A-PSS and D-PSS are shown in Figs. 2(a) and 2(b). Two kinds of GaNs were found on PSS. One (GaN I) was initiated from *c*-plane of A-PSS and D-PSS. The other (GaN II) was from sidewall

surfaces of A-PSS [Figs. 2(a)]. Most of threading dislocations were initiated from *c*-plane. This is because most of the growth of GaN was initiated from *c*-planes.^{14,15} To realize the crystallographic relationships among GaN and sapphire substrate, selected area diffraction (SAD) patterns were taken from GaN I, GaN II, and PSS [Figs. 2(c)–2(f)]. GaN I was wurtzite structure as shown in Fig. 2(c). The crystallographic relationship between GaN I and sapphire is established as $(0001)_{\text{GaN I}} \parallel (0001)_{\text{sapphire}}$ and $[\bar{1}100]_{\text{GaN I}} \parallel [11\bar{2}0]_{\text{sapphire}}$. This orientation relationship is usually seen in the case of a GaN epitaxially grown on a *c*-plane sapphire. On the other hand, it is worthy to note that GaN II was zinc blende structure as shown in Fig. 2(c). There is no obviously crystallographic relationship between GaN II and sapphire substrate. The HRTEM images of zinc blende region (GaN II) and wurtzite region (GaN I) are shown in Figs. 2(g) and 2(h).

In addition to TEM, two other ways was used to evaluate the GaN crystal quality: (1) x-ray diffraction (XRD) and (2) screw dislocation density, which can be characterized by etching pit density (EPD). They are summarized in Table I. XRD shows that the full-width at half-maximum (FWHM) of the rocking curve decreases monotonically as the slanted angle is decreased from 57.4° to 31.6° for both the symmetric (002) and asymmetric (102) reflections. This indicates the structural quality of PSS-LEDs increased with decrease in slanted angle.¹⁶ The improvement on structural quality was also verified by EPD. Samples were etched in 210°C H_3PO_4 for 2 min. As expected, the EPD was reduced from 4.31×10^7 to $0.52 \times 10^7 \text{ cm}^{-2}$ when the slanted angle decreased from 57.4° to 31.6° . The reduction of dislocation density also indicated that the IQE was improved.¹⁷

We believe that the observed differences in EPDs/crystal qualities were due to the change in lateral growth area of GaN. Most of the growth of GaN was initiated not from sidewall surfaces but *c*-planes.^{14,15} There were following two kinds of *c*-planes: (1) top *c*-plane and (2) bottom *c*-plane. As the growth time growth time increased, GaN epilayers on the bottom *c*-plane covered these pyramids by lateral growth, which is similar to the ELOG mode.^{14,15}

The lateral growth area fraction (LGA) can be estimated by the following equation:

$$\text{LGA} = [1 - (c\text{-plane areas/total areas)}],$$

where *c*-plane areas include top and bottom *c*-plane areas. As listed in Table I, LGAs of LEDs indeed increased with decrease in slanted angle. As a result, the EPDs on the surfaces of LEDs decreased with slanted angle. This indicates that the

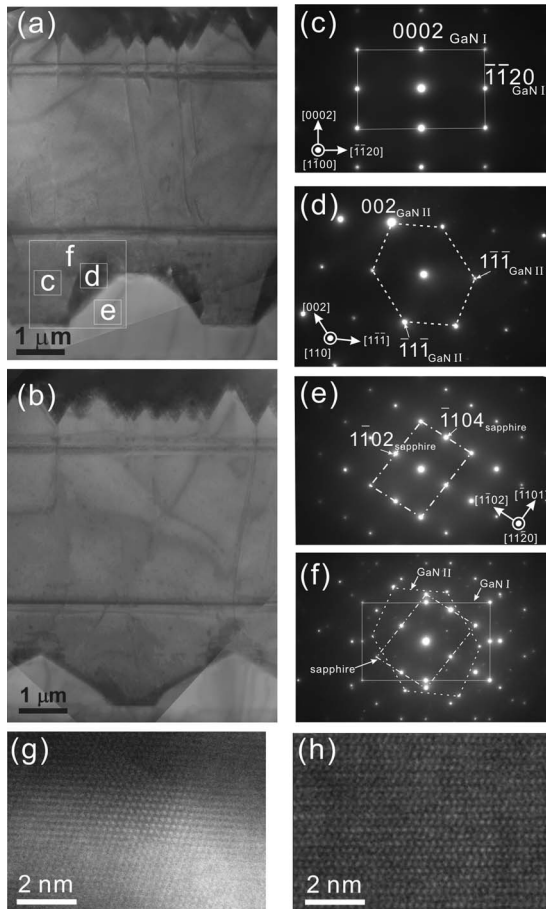


FIG. 2. Bright-field TEM images of (a) A-PSS and (b) D-PSS. (c), (d), (e), and (f) are SAD patterns taken from (a) A-PSS. These patterns are from GaN I[(c)], GaN II[(d)], sapphire substrate[(e)], and interface region [(f)] among GaN I, GaN II, and sapphire substrate. (g) and (h) are HRTEM images of (g) GaN II region (zinc blende structure) and (h) GaN I region (wurtzite structure).

GaN crystal quality improved with decrease in slanted angle.

The other factor might affect the light intensity and the output power is the light extraction efficiency. Monte Carlo simulation reveals that the extraction efficiency were increased when the slanted angle was decreased from 80° to 30°. ¹⁸ As a result, the light extraction efficiencies of PSS-LEDs increased as the slanted angle was decreased from 57.4° to 31.6°.

In summary, periodic triangle pyramidal array PSSs with various slanted angles were fabricated by wet etching. Beside normal wurtzite GaN, zinc blende GaN was found on the sidewall surfaces (*r*-planes) of A-PSS. The luminescence intensity, the output power, crystal quality, and light extraction efficiencies of PSS-LEDs increased as the slanted angle was decreased from 57.4° (*r*-plane) to 31.6°. We believe that these observed differences were due to the change in lateral growth area of GaN, which increased with decrease in slanted angle. When the angle decreased to 31.6°, the light intensity and the output power of D-LED were 140.0 mcd and 20.8 mW, which were 1.54 and 1.37 times higher than those of A-LED.

This project was funded by Epistar Corporation, Sino American Silicon Products Incorporation, and the National Science Council of the Republic of China under Grant No. 98-2221-E009-041-MY3. Technical supports from the National Nano Device Laboratory, Center for Nano Science and Technology, Nano Facility Center and Semiconductor Laser Technology Laboratory of the National Chiao Tung University are also acknowledged.

- ¹H. Amano, N. Sawaki, I. Akasaki, and Y. Toyoda, *Appl. Phys. Lett.* **48**, 353 (1986).
- ²K. Linthicum, T. Gehrke, D. Thomson, E. Carlson, P. Rajagopal, T. Smith, D. Batchelor, and R. Davis, *Appl. Phys. Lett.* **75**, 196 (1999).
- ³A. Sakai, H. Sunakawa, and A. Usui, *Appl. Phys. Lett.* **71**, 2259 (1997).
- ⁴W. C. Peng and Y. C. Sermon Wu, *Appl. Phys. Lett.* **88**, 181117 (2006).
- ⁵C. E. Lee, Y. J. Lee, H. C. Kuo, M. R. Tsai, B. S. Cheng, T. C. Lu, S. C. Wang, and C. T. Kuo, *IEEE Photon. Technol. Lett.* **19**, 1200 (2007).
- ⁶H. W. Huang, C. H. Lin, C. C. Yu, B. D. Lee, C. H. Chiu, C. F. Lai, H. C. Kuo, K. M. Leung, T. C. Lu, and S. C. Wang, *Nanotechnology* **19**, 185301 (2008).
- ⁷Y. C. Sermon Wu, C. Liao, and W. C. Peng, *Electrochem. Solid-State Lett.* **10**, J126 (2007).
- ⁸D. S. Wu, W. K. Wang, K. S. Wen, S. C. Huang, S. H. Lin, R. H. Hrong, Y. S. Yu, and M. H. Pan, *J. Electrochem. Soc.* **153**, G765 (2006).
- ⁹J. H. Lee, J. T. Oh, Y. C. Kim, and J. H. Lee, *IEEE Photon. Technol. Lett.* **20**, 1563 (2008).
- ¹⁰C. H. Chiu, H. H. Yen, C. L. Chao, Z. Y. Li, Yu. Peichen, H. C. Kuo, T. C. Lu, S. C. Wang, K. M. Lau, and S. J. Cheng, *Appl. Phys. Lett.* **93**, 081108 (2008).
- ¹¹H. C. Lin, R. S. Lin, J. I. Chyi, and C. M. Lee, *IEEE Photon. Technol. Lett.* **20**, 1621 (2008).
- ¹²F. Dwikusuma, D. Saulys, and T. F. Kuech, *J. Electrochem. Soc.* **149**, G603 (2002).
- ¹³H. Gao, F. Yan, Y. Zhang, J. Li, Y. Zeng, and G. Wang, *J. Appl. Phys.* **103**, 014314 (2008).
- ¹⁴C.-C. Pan, C.-H. Hsieh, C.-W. Lin, and J.-I. Chyi, *J. Appl. Phys.* **102**, 084503 (2007).
- ¹⁵J. H. Lee, J. T. Oh, J. S. Park, J. W. Kim, Y. C. Kim, J. W. Lee, and H. K. Cho, *Phys. Status Solidi C* **3**, 2169 (2006).
- ¹⁶B. Heying, X. H. Wu, S. Keller, Y. Li, D. Kapolnek, B. P. Keller, S. P. DenBaars, and J. S. Speck, *Appl. Phys. Lett.* **68**, 643 (1996).
- ¹⁷Q. Dai, M. F. Schubert, M. H. Kim, J. K. Kim, E. F. Schubert, D. D. Koleske, M. H. Crawford, S. R. Lee, A. J. Fischer, G. Thaler, and M. A. Banas, *Appl. Phys. Lett.* **94**, 111109 (2009).
- ¹⁸T. X. Lee, K. F. Gao, W. T. Chien, and C. C. Sun, *Opt. Express* **15**, 6670 (2007).